Tetrahedron Vol. 50, No. 1, pp. 77-92, 1994
Printed in Great Britain

0040-4020/94 $6.00+.00

CONFORMATIONAL ANALYSIS OF THE CARBOHYDRATE PORTION OF T AND T_N HAPTENS BY NMR SPECTROSCOPY AND MOLECULAR MODELING

Stephen Hanessian[a,*], Hiroshi Hori[a], Yongxue Tu[a,b,c] and Yvan Boulanger[b,c]

a. Department of Chemistry and b. Research Group on Membrane Transport,
Université de Montréal, C.P. 6128, Succ. A, Montreal, Quebec H3C 3J7 (Canada)

c. INRS-Santé, Université du Québec, 245 Hymus Blvd., Pointe-Claire,
Quebec H9R 1G6 (Canada)

Key words: Carbohydrate, hapten, NMR, three-dimensional structure, molecular modeling.

Abstract: *The conformations of the crotyl derivatives of the T (β-D-Gal(1→3)-Crotylα-D-GalNAc) and T_N (Crotylα-D-GalNAc) haptens as well as of Meβ-D-Gal were investigated in D_2O, DMSO-d_6 and 85% H_2O: 15% acetone-d_6 using ^1H and ^{13}C NMR spectroscopy and molecular modeling. The two sugar moieties are in a $^4C_1$ conformation and they adopt a quasi-parallel orientation in the T hapten, with hydrogens H1' and H3 being in close proximity. The hydroxymethyl chains adopt a* gt *conformation, the NH and H2 are antiperiplanar whereas the crotyl chain displays significant segmental mobility. Vicinal coupling constants of hydroxyl protons and saturation transfer rates in aqueous media indicate that the hydroxyl groups are relatively mobile except for OH2' which probably forms a weak hydrogen bond with the amide nitrogen. An energy-minimized molecular model consistent with all the NMR data could be constructed and areas favorable to hydrophilic interactions could be determined. Except for the rotamer distribution of the hydroxymethyl group, the conformations are very similar in all three solvents.*

INTRODUCTION

The T and T_N antigenic determinants are carbohydrate structures existing on the N-terminal part of glycophorin A, a major transmembrane glycoprotein found in human erythrocytes and responsible for MN blood group specificity (1). These haptens have also been found on the surface of human carcinoma cells (2-4) and are known as stage-specific differentiation antigens in human fetuses (5). The chemical structure of the T hapten consists of a disaccharide corresponding to β-D-Gal(1→3)-Serα-D-GalNAc or β-D-Gal(1→3)-Thrα-D-GalNAc (6) whereas the T_N hapten is a monosaccharide corresponding to Serα-D-GalNAc or Thrα-D-GalNAc (7).

The first synthesis of the disaccharide β-D-Gal(1→3)-α-D-GalNAc was carried out by Flowers and Shapiro in 1965 (8) and was followed by several syntheses of β-D-Gal(1→3)-Serα-D-GalNAc and β-D-Gal(1→3)-Thrα-D-GalNAc (9-11) and of Serα-GalNAc and Thrα-GalNAc (12,13). Polyglycosylated N-terminal oligopeptides of glycophorin A (14-16), artificial T and T_N antigenic determinants as well as haptens with linkers (17-20) have been recently synthesized. The syntheses of the crotyl derivatives of the T and T_N haptens **1** and **2** have also been performed independently in our laboratory (21).

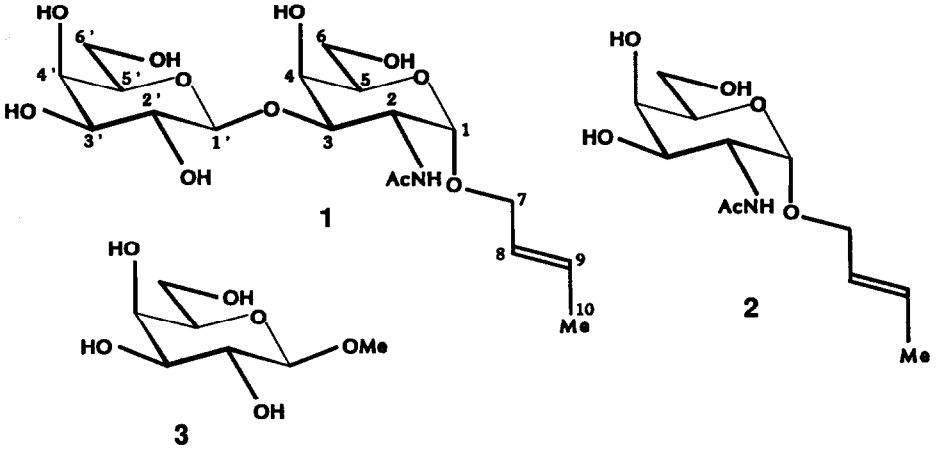

Conformational studies using NMR spectroscopy (22) and theoretical calculations have already been reported for saccharide and glycopeptide structures related to the T and T_N haptens (23-28). Among the structures related to the T hapten, studies of the β-D-Gal(1→3)-Bnα-D-GalNAc disaccharide as a constituting unit of antifreeze glycoproteins from polar fish (25,27), of the β-D-Gal(1→3)-Bnα-D-GalNAc disaccharide linked to a pentapeptide existing in glycophorin A_M and A_N (23,28), of the β-D-Gal(1→3)-Meα-D-GalNAc disaccharide (26) and of the β-D-Gal(1→3)-Prβ-D-GalNAc (β- instead of α-D-GalNAc in **1**) free and linked to the pentasaccharide portion of gangliosides G_{M2} and G_{M1} (29) have been reported. Investigated structures related to the T_N hapten include the 3-OMe-Meα-D-GalNAc (25), the α-D-GalNAc monosaccharide linked to a pentapeptide existing in glycophorin A_M and A_N (23,28) and the Meα-D-GalNAc (26). Besides providing partial or full ^1H and ^{13}C chemical shift assignments, these studies have shown consistent $^4C_1$ sugar ring conformations and proximity of the H1' and H3 protons. NMR and molecular modeling studies of glycopentapeptides have demonstrated that different glycosidic structures could be obtained depending on the point of attachment to the peptide chain (23,28). *Although the general features of the saccharide units have been defined, no molecular modeling and no information on the hydroxyl groups have been reported for the isolated mono- and disaccharides.*

In view of the importance of the T and T_N antigens as tumor markers (30) and their possible role in the recognition of specific antibodies and related biologically important proteins at the molecular level, we undertook a detailed study of the conformation of model glycosides **1** and **2** by NMR spectroscopy and molecular modeling. The conformations of the synthetic β-D-Gal(1→3)-Crotylα-D-GalNAc **1** and Crotylα-D-GalNAc **2**, models of the naturally occurring T and T_N haptens respectively, as well as that of the Meβ-D-Gal **3** were investigated in three different solvents (DMSO-d_6, D_2O and 85% H_2O: 15% acetone-d_6) using ^1H and ^{13}C NMR spectroscopy, energy minimization and calculation of energetically favorable binding sites. Chemical shifts, coupling constants, n.O.e. measurements and temperature dependences of the chemical shifts of the exchangeable protons were used to determine the conformations of the sugar rings, the configuration of the glycosidic linkages, the relative orientations of the hydroxyl groups and their exposure to the solvent. Energy minimized structures consistent with all NMR data could be calculated by molecular modeling.

RESULTS AND DISCUSSION

The conformational structure of **1** (T hapten model) as well as those of compounds **2** (T_N hapten model) and **3**, which represent the left and right hand sugar portions of **1**, respectively, have been determined by NMR spectroscopy, analyzing their different constituting groups: the glycosidic linkages, the hydroxymethyl, N-acetyl, *E*-crotyl and hydroxyl groups. Subsequently, molecular modeling was used to derive optimized structures.

I. NMR results

Hexose conformation

The ^1H and ^{13}C chemical shifts and coupling constants of **1** and **2** measured in three different solvents, D_2O, DMSO-d_6 and 85% H_2O: 15% acetone-d_6, are given in Tables I, II and III. The comparison of these NMR data with literature values of related compounds studied in D_2O (13,25-28,31,32) shows an excellent agreement and indicates that all hexose units adopt a $^4C_1$ conformation. The practically unchanged coupling constants and the consistent upfield shifts in DMSO-d_6 and 85% H_2O: 15% acetone-d_6 suggests that the same sugar ring conformation is present in the three solvents.

β(1→3) Glycosidic linkage

The conformation of the β(1→3) glycosidic linkage of **1** was analyzed on the basis of n.O.e. and $^3J_{CH}$ values (Tables IV and V). When H1' was irradiated, a relatively strong n.O.e. effect was observed for H3, but very little and no enhancements were observed for H2 and H4, respectively (Table IV). The intensity of the observed n.O.e. of H3 was larger than the average n.O.e. value of H3' and H5', whose signals are overlapping in D_2O, suggesting that the H1'-H3 distance is smaller than the H1'-H3' or the

Table I. ^{1}H NMR Chemical Shifts of **1** and **2** in Different Solvents

Residue	Proton	Chemical shifts (ppm)					
		D_2O		DMSO-d_6		H_2O-acetone-d_6[a]	
		1	**2**	**1**	**2**	**1**	**2**
GalNAc	H1	4.946	4.942	4.696	4.654	4.792	4.746
	H2	4.336	4.145	4.185	4.031	4.191	4.020
	H3	4.033	3.889	3.739	3.592	3.879	3.745
	H4	4.252	3.98[b]	3.914	3.713	4.108	3.843
	H5	4.019	3.96[b]	3.595	3.580	3.853	3.800
	H6a[c]	3.775	3.762	3.45[b]	3.461	3.641	3.629
	H6b[c]	3.757	3.748	3.50[b]	3.509	3.612	3.608
Gal	H1'	4.478		4.348		4.336	
	H2'	3.535		3.310		3.392	
	H3'	3.638		3.231		3.487	
	H4'	3.924		3.601		3.772	
	H5'	3.674		3.349		3.521	
	H6a'[c]	3.780		3.45[b]		3.620	
	H6b'[c]	3.751		3.50[b]		3.592	
Crotyl	H7a	4.162	4.139	4.016	4.009	4.009	4.010
	H7b	3.984	3.957	3.802	3.815	3.828	3.980
	H8	5.645	5.615	5.543	5.521	5.478	5.471
	H9	5.868	5.837	5.745	5.687	5.704	5.683
	H10	1.726	1.706	1.656	1.661	1.576	1.564
Acetyl	CH_3	2.040	2.041	1.799	1.826	1.889	1.927
	NH			7.680		7.915	7.830

All data were recorded at 21°C. [a] The solvent composition was 85% H_2O or D_2O: 15% acetone-d_6. [b] Exact values were not obtained due to overlap of the signals. [c] The assignment of H6*proR* and H6*proS* is described in the discussion.

H1'-H5' distance. This can be explained by the facts that the C-O bond length is smaller than the C-C bond length and that geometric parameters are different. Similarly strong n.O.e. effects between H1' and H3 have been reported for β-D-Gal(1→3)-Bnα-D-GalNAc (25), β-D-Gal(1→3)-Prβ-D-GalNAc (29) and the antifreeze glycoprotein in D_2O (25). These data indicate that the largely dominant conformation around the glycosidic linkage is one in which H3 and H1' are in close proximity, and in which the N-acetyl group of α-D-GalNAc and the hydroxymethyl group of β-D-Gal are on opposite sides of the molecule in aqueous and DMSO solutions (see Molecular modeling section).

Table II. ^{1}H NMR Coupling Constants of **1** and **2** in Different Solvents

Residue	Protons	Coupling constants (Hz)					
		D_2O		DMSO-d_6		H_2O-acetone-d_6[a]	
		1	**2**	**1**	**2**	**1**	**2**
GalNac	H1,H2	3.8	3.8	3.5	3.6	3.8	3.7
	H2,H3	11.1	11.1	11.2	11.1	11.1	11
	H3,H4	3.2	3.3	3.2	3.3	3.0	3.2
	H4,H5	0.7	0.9	1	1[b]	1[b]	1[b]
	H5,H6a	7.7	8	5-7[b]	6.5	6.0	6.3
	H5,H6b	4.8	4.3	5-7[b]	6.0	6.3	6.3
	H6a,H6b	11.8	11.7	11[b]	10.9	11	12
	H1,H4	0.5			0.5		
Gal	H1',H2'	7.9		7.3		7.7	
	H2',H3'	10.0		9.5		10.0	
	H3',H4'	3.5		3.2		3.3	
	H4',H5'	0.9		1		0.8	
	H5',H6a'	7.8		5-7		5.4	
	H5',H6b'	4.3		5-7		7.0	
	H6a',H6b'	11.9		11[b]		11	
Crotyl	H7a,H7b	12.0	12.0	12.4	12.5	12.0	13
	H7a,H8	6.0	6.0	5.5	5.8	5.9	5.7
	H7b,H8	7.2	7.2	6.4	6.5	7.1	7.4
	H8,H9	15.4	15.4	15.3	15.3	15.3	15.3
	H9,H10	6.5	6.5	6.3	6.3	6.5	6.5
	H7a,H9						
	H7b,H9						
	H7a,H10	1-1.5					
	H7b,H10						
	H8,H10						
	H2,NH			8.2		9.4	9

All data were recorded at 21°C. [a] The solvent composition was 85% H_2O or D_2O: 15% acetone-d_6. [b] Exact values were not obtained due to overlap of the signals.

^{13}C-^{1}H coupling constants were measured using the selective CH J-resolved method (32) and used to calculate the glycosidic dihedral angles ϕ' and ψ' using Tvaroška's equation and assuming the presence of a single conformer (33). Dihedral angles ϕ' ranged between +23° and +29° in the three solvents and ψ' values were -16° and -20°, respectively, in D_2O and DMSO-d_6 (Table V). Negative and positive signs for the ϕ' and ψ' angles were determined by considering the exo-anomeric effect

Table III. ^{13}C NMR Chemical Shifts and NT_1 Values of **1** and **2**

Residue	Carbon	Chemical shifts (ppm)						NT_1 (s)[a]
		D_2O		DMSO-d_6		D_2O-acetone-d_6		D_2O
		1	**2**	**1**	**2**	**1**	**2**	**1**
GalNAc	C1	96.92	96.73	96.48	96.33	96.46	96.23	0.28
	C2	49.48	50.76	48.61	49.83	49.01	50.35	0.28
	C3	78.16	68.56	75.88	67.55	77.67	68.19	0.31
	C4	69.60	69.34	67.49	68.24	69.02[b]	68.91	0.31
	C5	71.46	71.79	71.40	71.38	70.93	71.2	0.31[c]
	C6	62.04	62.07	60.74[d]	60.75	61.52[e]	61.56	0.48
Gal	C1'	105.57		103.89		104.83		0.32
	C2'	71.46		70.84		71.15		0.31[c]
	C3'	73.37		73.42		73.09		0.31
	C4'	69.44		68.2		69.05[b]		0.31
	C5'	75.83		75.45		75.31		0.31
	C6'	61.8		60.65[d]		61.38[e]		0.48
Crotyl	C7	69.23	69.31	67.19	66.98	68.59	68.61	0.62
	C8	126.78	126.70	127.58	127.68	126.35	126.27	1.17
	C9	132.65	132.71	128.70	128.31	131.74	131.78	1.10
	C10	17.97	17.95	17.65	17.67	17.36	17.44	7.35
Acetyl	CH_3	22.86	22.76	22.85	22.80	22.43	22.33	3.9
	C=O	175.39	175.40	169.93	169.67	174.57	174.56	

All data were obtained at 75.4 MHz and 21°C. [a]Measured by inversion-recovery method. [b, d,e] Interchangeable values. [c]Average value due to overlap of the signals.

(34) and the results of molecular modeling. The other solution of Tvaroška's equation giving angles of the order of ±140-150° could be eliminated considering steric hindrance and the n.O.e. results.

Hydroxymethyl groups

The assignment of prochiral protons H6R(H6*proR*) and H6S(H6*proS*) of individual hexose units in **1** and **2** in D_2O was based on the data of Ohrui *et al.* (26) who established the assignment using stereospecifically deuterated sugars. In DMSO-d_6, the H6 signals at lower and higher field were tentatively assigned to H6*proS* and H6*proR*, respectively. This is based on a report that H6S of Meα-D-Gal and Meβ-D-Gal resonates at lower field than H6R in DMSO-d_6, unlike in D_2O solution (35).

Table IV. ^1H-^1H n.O.e. Data and Calculated Interproton Distances for **1** in D_2O

Irradiated proton(s)	Affected proton(s)	n.O.e value (%)	Calculated distance (Å)[a]
H1	H2	36	2.37
	H7a	14	2.78
	H7b	4	3.42
	H8	4	3.42
	H9	4	3.42
H3,H5,H7b	H8	2	
	H9	3	
	H10	<1	
	H1'	9	
H4	H3,H5	28	2.77[b]
	H6a,H6b	6	
	H1'	<1	
H1'	H3	18	2.66
	H4	<1	
	H2'	6	3.19
	H3',H5'	26	2.81[b]
H2',H3'(partly)	H2	<1	
	H4	<1	
	H1'	5	
	H4'	3	

[a] Interproton distances were calculated from the relative n.O.e. using the reference value of 2.37 Å measured between H1 and H2 in a $^4C_1$ conformation. [b] Calculated assuming equidistant protons.

The rotamer distributions of C5-C6 and C5'-C6' single bonds were calculated by using three Karplus-type equations based on $^3J_{5,6R}$, $^3J_{5,6S}$, $^3J_{5',6R'}$ and $^3J_{5',6S'}$ coupling constant values (Table VI). The most favorable rotamer of the hydroxymethyl groups in **1** and **2** was *gt* (dihedral angle O5-C5-C6-C4 ca. 180°) (50-70%) in D_2O, the distribution of the minor rotamers *gg* and *tg* being 15-25%. A predominance of the *gt* conformer was also reported in D_2O for Meα-D-GalNAc, Meβ-D-GalNAc and β-D-Gal(1→3)-Meα-D-GalNAc (24) and in the solid state for **3** on the basis of neutron diffraction measurements (36). In D_2O, however, the conformation of **3** was predominantly *gg* (35). In DMSO-d_6, our data show no conformational preference, the ratio of *gg*:*gt*:*tg* being ca. 20:40:40 for **2** (Table VI). Little difference in this ratio is calculated if the assignment of H6R and H6S is reversed (ca. 20:35:45). A similar rotamer distribution has been reported for **3** in DMSO-d_6 (35). The rotamer distribution of C5-C6

Table V. ^{13}C-^{1}H Coupling Constants and Calculated Torsion Angles of **1**

Solvent	$^{3}J_{CH}$ Coupling constant (Hz)	Torsion angles (°)	
		Calculated from $^{3}J_{CH}$[a]	Molecular model
D_2O	$J_{1',3} = 5.2$ $J_{3,1'} = 4.6$ $J_{7,1} = 4.0$	$\psi' = -16$ $\phi' = +26$ $\phi = -33$	-17.5 +27.8 -40.6
DMSO-d_6	$J_{1',3} = 5.0$ $J_{3,1'} = 4.8$	$\psi' = -20$ $\phi' = +23$	
H_2O:acetone-d_6	$J_{3,1'} = 4.3$	$\phi' = +29$	

All coupling constants were measured using ^{13}C J-resolved spectroscopy at 26°C (D_2O), 30°C (DMSO-d_6) and 21°C (85% H_2O: 15% acetone-d_6). [a]Calculated as single conformer using Tvaroška's equation $^{3}J_{CH} = 5.7\cos^2\theta - 0.6\cos\theta + 0.5$ (33). The signs of the angles are given on the basis of the conformations calculated by molecular modeling.

and C5'-C6' of **1** in DMSO-d_6 was estimated to be similar to that of **2** and **3** although the coupling constants and the chemical shifts of these prochiral protons could not be obtained precisely because of peak overlapping and broadening. The nature of the solvent seems therefore to affect the rotamer distribution of the hydroxymethyl groups in these molecules.

Table VI. Rotamer Distributions of the C5-C6 and C5'-C6' Bonds

		Rotamer distributions (%)[a]											
		$^{3}J_{5,6R}$ $^{3}J_{5',6R'}$	$^{3}J_{5,6S}$ $^{3}J_{5',6S'}$	Equation A			Equation B			Equation C		
Solvent	Compound	(Hz)	(Hz)	*gg*	*gt*	*tg*	*gg*	*gt*	*tg*	*gg*	*gt*	*tg*
D_2O	**1**	7.7	4.8	22	51	27	17	60	23	16	59	25
		7.8	4.3	22	54	22	16	67	17	19	62	19
	2	8.2	4.3	21	58	21	16	68	16	14	66	20
DMSO-d_6	**2**	6.5	6.0	26	33	41	20	41	39	20	42	38
	2[b]	6.0	6.5	28	26	46	21	33	46	22	34	44

[a]All data were recorded at 21°C. Rotamer distributions were calculated using equation A (38), B (39) or C (35). [b]Calculated using a reversed assignment of H6R and H6S.

α-Glycosidic linkage, E-crotyl and N-acetyl groups

There is no evidence of significant conformational difference between the N-acetyl groups in **1** and **2**. Relatively large coupling constant values between H2 and NH (8.2-9.5 Hz) in **1** and **2** are indicative of an antiperiplanar relationship between the two protons (Table VII). The ^1H chemical shift of NH and the ^{13}C chemical shift of the carbonyl are very similar for these two glycosides (Tables I-III).

Table VII. ^1H NMR Chemical Shifts and Coupling Constants of the Hydroxyl and Amide Protons of **1**, **2** and **3**

Residue	Proton	Chemical shifts (ppm)					
		DMSO-d_6, 21°C			H_2O-acetone-d_6, -12°C		
		1	**2**	**3**	**1**	**2**	**3**
GalNAc	NH	7.564	7.618		8.236	8.235	
	OH3	4.398				5.878	
	OH4	4.296	4.526		5.843	5.942	
	OH6	4.587	4.568		5.928	5.947	
Gal	OH2'	4.296		4.892	6.069		6.428
	OH3'	4.753		4.693	5.982		6.016
	OH4'	4.368		4.337	5.811		5.795
	OH6'	4.577		4.561	6.070		6.021

Residue	Protons	Coupling constants (Hz)					
		DMSO-d_6, 21°C			H_2O-acetone-d_6, -12°C		
		1	**2**	**3**	**1**	**2**	**3**
GalNAc	NH,H2	8.2	8.4		9.5	9.1	
	OH3,H3		7.0			6.0	
	OH4,H4	4.4	4.5		3.6	4.5	
	OH4,H5	0.6[a]	0.6				
	OH6,H6a	5.6	5.2		5.0	[b]	
	OH6,H6b	5.6	6.1		5.0	[b]	
Gal	OH2',H2'	3.5		4.6	4.0		3.5
	OH3',H3'	5.5		5.4	5.0		[b]
	OH4',H4'	4.4		4.6	5.0		5.0
	OH4',H5'	0.6[a]		0.6			
	OH6',H6a'	5.6		5.2			[b]
	OH6',H6b'	5.6		6.1			[b]

[a] Values measured at 40°C. [b] Not measurable due to overlap of signals.

Saturation of H1 gave rise to n.O.e. effects on H7a, H7b, H8 and H9 (Table IV) in the *E*-crotyl group. The n.O.e. effects between H1 and H7a or H7b are smaller than those observed between H1' and H3 and suggest that they are not in the same proximity probably as a result of greater chain mobility. This is consistent with the ^{13}C NT_1 values showing evidence of considerable segmental mobility in the *E*-crotyl chain (Table III). The conformation of the corresponding α-glycosidic linkage is dependent on the nature of the group attached and has been shown to differ for glycosides attached to the same residues in different positions of a peptide chain (23).

Hydroxyl and amide groups

The ^1H NMR signals of all hydroxyl and amide protons of **1**, **2** and **3** were observable in DMSO-d_6 at 21°C and in 85% H_2O: 15% acetone-d_6 at -12°C using solvent suppression (Table VII and Fig. 1). One- and two-dimensional NMR spectra were acquired using the 1-5.4-5.4-1 jump-return sequence for solvent suppression (Figs. 1 and 2). The chemical shifts for these groups are very similar between **1** and **2** and between **1** and **3**, except for OH2' and to a lesser extent OH4 (Table VII). Solvent effects on all chemical shifts are very large (0.6-1.5 ppm) as can be expected for such peripheral polar groups.

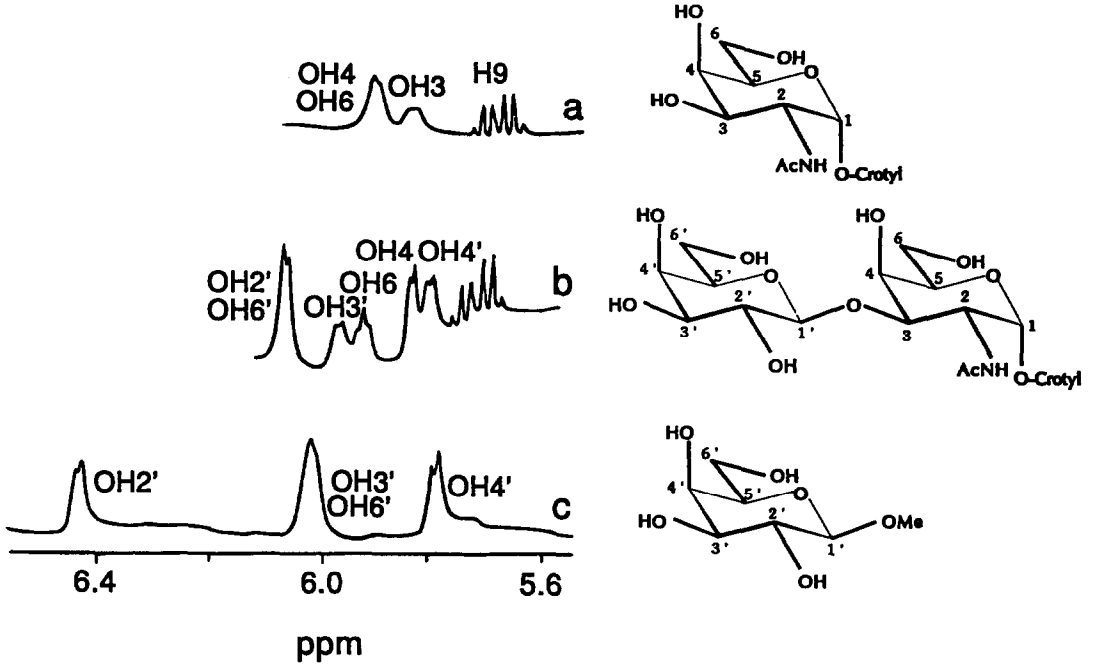

Fig. 1. Hydroxyl region of the ^1H NMR spectra of (a) **2**, (b) **1** and (c) **3** in 85% H_2O: 15% acetone-d_6 at 400 MHz. Spectra were acquired at -12°C using a 1-2τ-5.4-τ-5.4-τ-1-ACQ pulse sequence for water suppression.

Except in cases where signal overlap prevented their measurement, vicinal coupling constants could be determined for all OH groups (Table VII; Fig. 3). Long range coupling constants between OH4 and H5 and between OH4' and H5' could also be measured. Most vicinal CH-OH coupling constants ($^3J_{H,OH}$) values are in the range 5-6 Hz (Table VII). To our knowledge, no Karplus relationship has been developed for such hydroxyl systems. However, when comparing to other Karplus relationships, these medium-range values appear to be consistent with motional averaging, as would be expected of such peripheral groups. Lower values measured for OH4-H4, OH2'-H2' and OH4'-H4' could be indicative of involvement in hydrogen bonding. Small differences in coupling constants could be observed between the two solvents suggesting small structural variations between the two conditions.

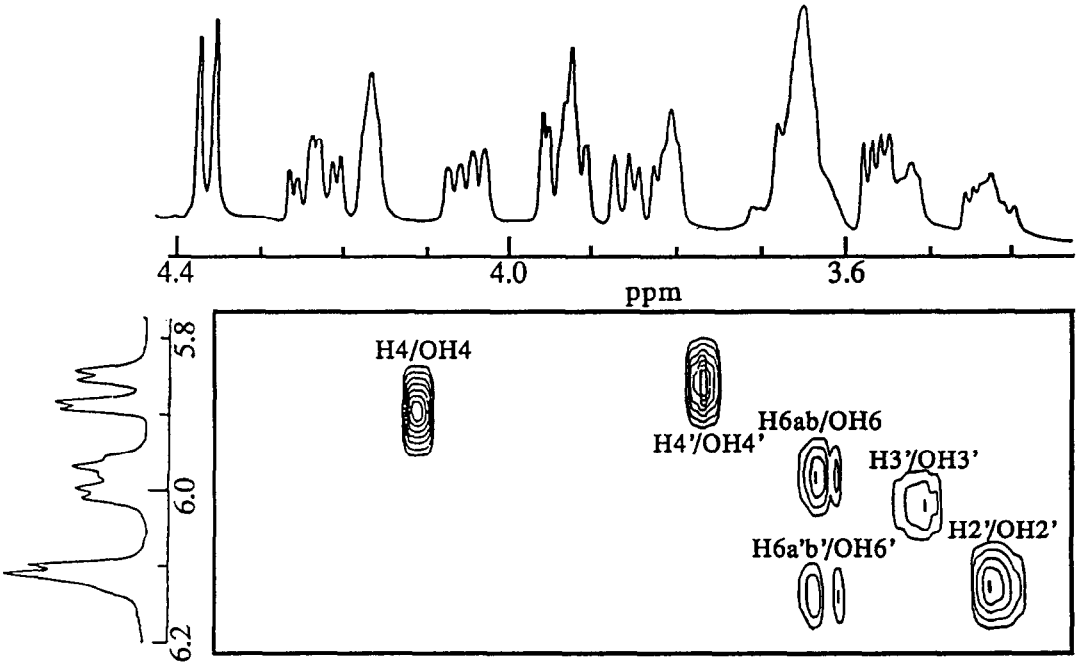

Fig. 2. Hydroxyl-CH region of the COSY spectrum of **1** in 85% H_2O: 15% acetone-d_6 acquired at 400 MHz using solvent suppression at a temperature of -12°C.

The temperature dependence of the chemical shifts of all hydroxyl and amide protons of **1** were determined in DMSO-d_6 (Table VIII). Except for OH2', all values are smaller than -5 x 10^{-3} ppm/°C and are not indicative of any involvement in intramolecular interactions such as hydrogen bonding. The value of -4.0 x 10^{-3} ppm/°C measured for OH2' suggests that this group is less exposed to the solvent as a result of hydrogen bonding (although not very strong). This conclusion is consistent with the saturation transfer experiments which show that the least affected proton following H_2O saturation is OH2' (Fig. 3). In contrast, the most affected protons are OH3', OH6 and OH6' whose signals practically disappear following saturation. These protons seem to be the most exposed to the solvent.

Table VIII. Temperature Dependence of the Chemical Shifts of the Hydroxyl and Amide Protons in DMSO-d_6[a]

Residue	Protons	$\Delta\delta/\Delta T$ (x 10^{-3} ppm/°C)		
		1	**2**	**3**
GalNAc	NH	-6.2	-7.0	
	OH3		-6.3	
	OH4	-6.6	-5.6	
	OH6	-5.7	-5.4	
Gal	OH2'	-4.0		-7.3
	OH3'	-7.1		-7.2
	OH4'	-5.7		-6.0
	OH6'	-5.2		-5.4

[a]Values measured between 20 and 60°C.

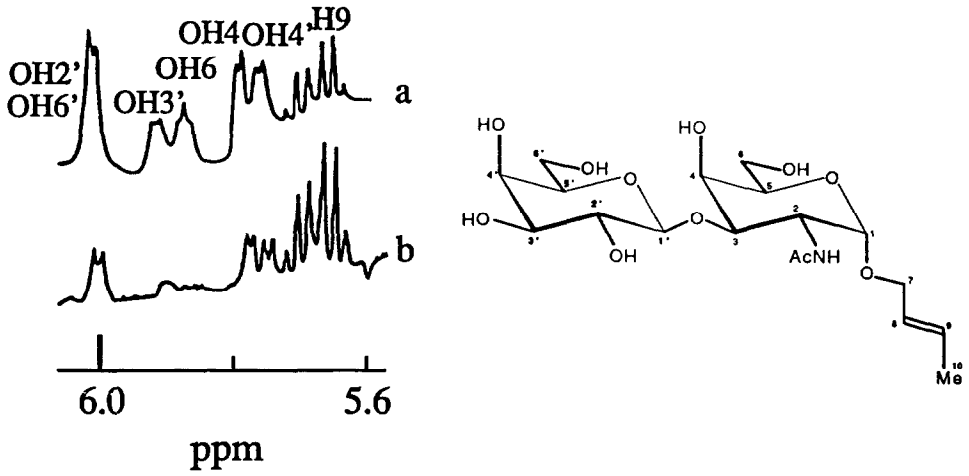

Fig. 3. Hydroxyl region of the ^{1}H NMR spectrum of **1** in 85% H_2O: 15% acetone-d_6 acquired at 400 MHz and at -12°C (a) without presaturation and (b) after 3.0 s presaturation of the water signal.

II. Molecular modeling

The molecular structure of **1** in water generated by molecular modeling using the NMR-derived torsion angle (Table V) and interproton distance (Table IV) constraints is illustrated in Fig. 4. In the energy minimized conformation, the relative orientation of the two sugar rings and the orientations of the N-acetyl and *E*-crotyl side chains are fixed by the NMR constraints. The hydroxymethyl groups, which were not submitted to any constraint, are both in a *gt* rotamer conformation, in agreement with

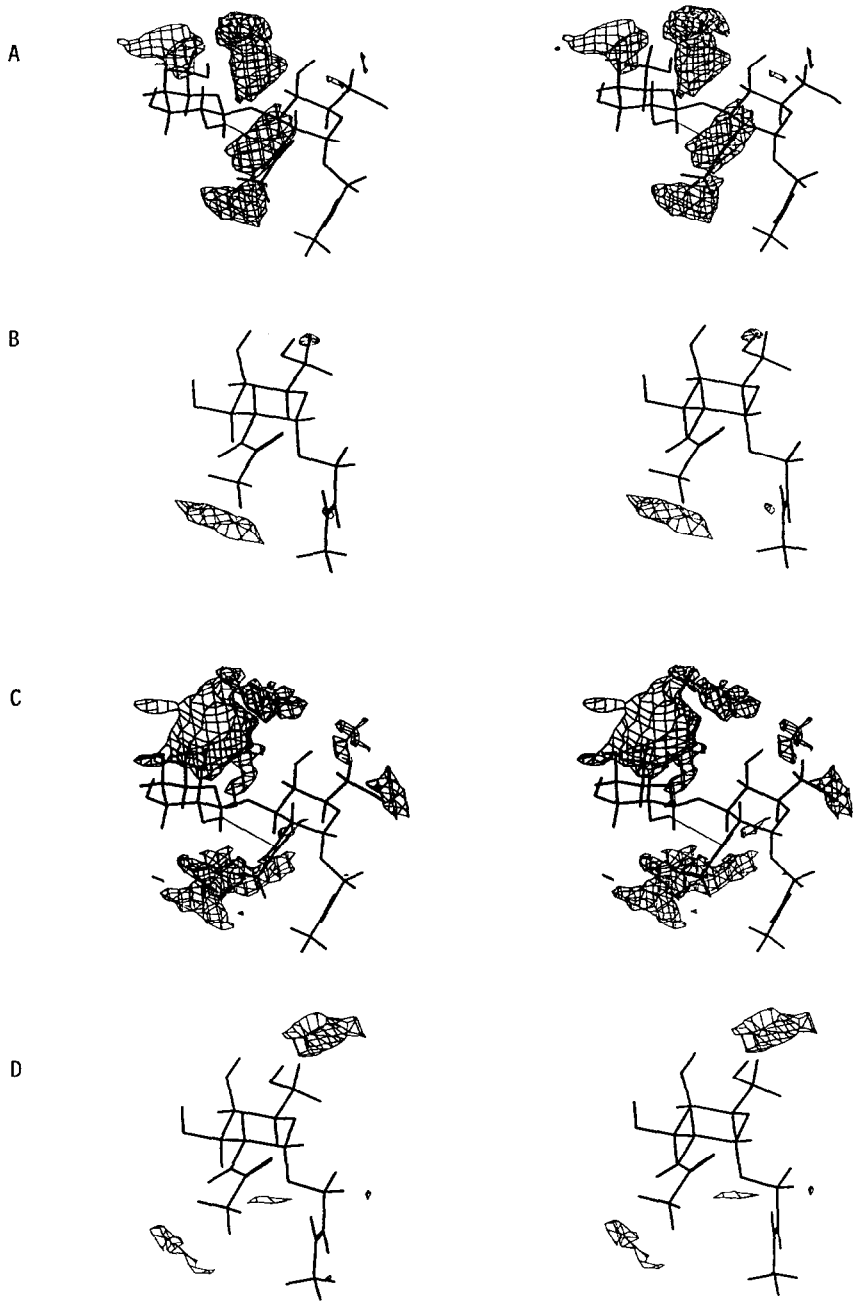

Fig. 4. Stereo views of the energy minimized structures **1** and **2** and their hydrophilic interactions (a) **1** with water, (b) **2** with water, (c) **1** with L-serine and (d) **2** with L-serine. The cutoff energies were (a) -7.5, (b) -7.5, (c)-20 and (d) -20 kcal/mol, respectively.

the calculation of the rotamer populations on the basis of coupling constants (Table VI). A weak hydrogen bond can be formed between the hydrogen of OH2' and the N-acetyl nitrogen, which are separated by 2.8 Å. This is consistent with the temperature dependence of the chemical shifts given in Table VIII.

Recently, the conformation of the N-terminal pentapeptide of glycophorin A_M and A_N bearing three T epitopes was reported based on molecular mechanics calculations and NMR data (23). The proposed conformations around the β(1→3)-D-Gal-α-D-GalNAc linkage in all but one of the disaccharide units were different from that found by our studies of **1** in solution. A different network of hydrogen bonding involving the peptide moiety was proposed. These data seem to suggest that the attachment of the haptens to the peptide chain may modify the conformation of the disaccharide relative to its conformation in solution.

We have performed a molecular interaction calculation for water and L-serine with the haptens **1** and **2** using the GRID program (40). The strongest interactions between water and **1** were located around the β(1→3) glycosidic linkage and above OH3' and OH4' (Fig. 4a). The interaction of water with **2** is much weaker at the same cutoff energy and occurs mostly around the N-acetyl amide (Fig. 4b). The interaction of L-serine with **1** occurs also around the glycosidic bond but it is stronger (lower cutoff energy) than with water and more evenly distributed above the β-D-Gal sugar ring (Fig. 4c). The interaction of **2** with L-serine occurs predominantly with the upper surface of the molecule (Fig. 4d). Similar patterns of interaction were observed with other hydrophilic molecules (HCOOH, NH_3, CH_3OH). These data show that polar media interact much more strongly with the disaccharide **1** than with the monosaccharide **2**, the main interaction occurring around the glycosidic linkage.

CONCLUSION

Using NMR data and molecular modeling, a detailed chemical structure consistent with all the experimental data could be determined for the T hapten model **1** in aqueous medium. Both sugar rings adopt a parallel $^4C_1$ conformation, the *E*-crotyl and N-acetyl side chains are extended, the hydroxymethyl adopts a *gt* rotamer conformation and a hydrogen bond is formed between the OH2' and NH groups. Using the GRID program, we find that the hydrophilic interactions are maximal around the β(1→3) glycosidic linkage. For the T_N hapten model **2**, weaker hydrophilic interactions are observed with the lower or upper surfaces of the molecule. In other solvents and in constituting monosaccharides **2** and **3**, NMR data indicate that the same conformation exists, except for the hydroxymethyl rotamer distribution which becomes predominantly *dg* in DMSO.

ACKNOWLEDGMENTS

The authors would like to thank the Fonds de la Recherche en Santé du Québec for a chercheur-boursier fellowship (Y.B.) and the Research Group on Membrane Transport, Université de Montréal for a postdoctoral fellowship (Y.T.). They thank Dr. R. Koganty, Biomira (Edmonton, Alberta, Canada) for samples of **1** and **2** as reference materials.

EXPERIMENTAL

The synthesis of the crotyl derivatives of the T hapten **1**, β-D-Gal(1→3)-Crotylα-D-GalNAc (mp 228-230°C; $[\alpha]_D^{25}$ +114.4° (c 0.59, MeOH)) and of the T_N hapten **2**, Crotylα-D-GalNAc (mp 193-194°C; $[\alpha]_D^{25}$ +206.6° (c 1.02, MeOH)) will be described elsewhere. Deuterated solvents D_2O, acetone-d_6 and DMSO-d_6 were purchased from Merck, Sharp & Dohme Isotopes (Pointe-Claire, Canada). ^1H and ^{13}C NMR spectra were recorded at 299.95 and 75.43 MHz, respectively, on a Varian VXR-300 spectrometer or at 400.13 and 100.13 MHz, respectively on a Bruker WH-400 spectrometer at the Laboratoire Régional de RMN à Haut Champ, Université de Montréal. Spin-lattice relaxation time measurements were performed using the inversion-recovery technique. ^1H-^{13}C coupling constants were determined from CH J-resolved spectroscopy. Two-dimensional COSY and NOESY spectra were acquired in the absolute value mode using 1024 x 512 data points. Saturation transfer experiments were performed by the method of Forsén and Hoffman (37) using a 3.0 s presaturation pulse at the water frequency. Solvent suppression was accomplished using the 1-2τ-5.4-τ-5.4-2τ-1 pulse sequence.

Molecular modeling was performed using the InsightII and Discover softwares from Biosym Technologies Inc. operating on a Silicon Graphics Iris Indigo XS computer workstation. Distance and torsion angle constraints derived from NMR (Tables IV and V, except H1-H8 and H1-H9 distances due to their imprecision) were utilized in the energy minimization process with a force constant of 100 $kcal.mol^{-1}.Å^{-2}$. The Biosym CVFF force field and the conjugate gradient energy minimization algorithm were used. The structure was then refined in the water solvent environment. Analysis of the hydrophilic interactions between different media (water, L-serine, HCOOH, NH_3, CH_3OH) and molecules **1** and **2** was performed using the GRID program (Molecular Discovery Ltd.).

REFERENCES

1. Tomita, M.; Marchesi, V.T. *Proc. Natl. Acad. Sci. USA* **1975**, *72*, 2964-2968.
2. Springer, G.F.; Desai, P.R.; Banatwala, I. *J. Natl. Cancer Inst.* **1975**, *54*, 335-339.
3. Springer, G.F.; Murthy, M.S.; Desai, P.R.; Scanlon, E.F. *Cancer* **1980**, *45*, 2949-2954.
4. Springer, G.F.; Desai, P.R.; Murthy, M.S.; Scanlon, E.F. *J. Surg. Oncol.* **1979**, *11*, 95-106.
5. Springer, G.F.; Tegtmeyer, H.; Cromer, D.W. *Fed. Proc. Fed. Am. Soc. Exp. Biol.* **1984**, *43*, 1750.
6. Kim, Z.; Uhlenbruck, G. *Z. Immun. Forsch.* **1966**, *130*, 88-99.
7. Bird, G.W.G.; Shinton, N.K.; Wingham, J. *Br. J. Haematol.* **1971**, *21*, 443-453.
8. Flowers, H.M.; Shapiro, D. *J. Org. Chem.* **1965**, *30*, 2041-2043; for a recent synthesis, see Hedbys, L.; Johansson, E.; Mosbach, K.; Larsson, P.-O.; Gunnarsson, A.; Svensson, S. *Carbohydr. Res.* **1989**, *186*, 217-223.
9. Kaifu, R.; Osawa, T. *Carbohydr. Res.* **1979**, *69*, 79-88.
10. Paulsen, H.; Paal, M.; Schultz, M. *Tetrahedron Lett.* **1983**, *24*, 1759-1762.
11. Ferrari, B.; Pavia, A.A. *Carbohydr. Res.* **1980**, *79*, C1-C7.
12. Kaifu, R.; Osawa, T. *Carbohydr. Res.* **1977**, *58*, 235-239.
13. Paulsen, H.; Hölck, J.-P. *Carbohydr. Res.* **1982**, *109*, 89-107.
14. Ferrari, B.; Pavia, A.A. *Int. J. Peptide Protein Res.* **1983**, *22*, 549-559.
15. Bencomo, V.V.; Sinaÿ, P. *Carbohydr. Res.* **1983**, *116*, C9-C12.
16. Ferrari, B.; Pavia, A.A. *Tetrahedron* **1985**, *41*, 1939-1944.
17. Ratcliffe, R.M.; Baker, D.A.; Lemieux, R.U. *Carbohydr. Res.* **1981**, *93*, 35-41.
18. Paulsen, H.; Paal, M. *Carbohydr. Res.* **1984**, *135*, 71-84.
19. Kunz, H.; Birnbach, S.; Wernig, P. *Carbohydr. Res.* **1990**, *202*, 207-223.
20. Matta, K.L.; Barlow, J.J. *Carbohydr. Res.* **1976**, *48*, 65-71.
21. Hanessian, S.; Qui, D.; Lou, B. To be published.
22. Meyer, B. in *Topics in Current Chemistry*, **1990**, *154*, 142-208.
23. Pèpe, G.; Siri, D.; Oddon, Y.; Pavia, A.A.; Reboul, J.-P. *Carbohydr. Res.* **1991**, *209*, 67-81.
24. Nishida, Y.; Hori, H.; Ohrui, H.; Meguro, H. *Agric. Biol. Chem.* **1988**, *52*, 887-889.
25. Bush, C.A.; Feeney, R.E. *Int. J. Peptide Protein Res.* **1986**, *28*, 386-397.
26. Ohrui, H.; Nishida, Y.; Hori, H.; Meguro, H.; Zushi, S. *J. Carbohydr. Chem.* **1988**, *7*, 711-731.
27. Homans, S.W.; DeVries, A.L.; Parker, S.B. *FEBS Lett.* **1985**, *183*, 133-137.
28. Pavia, A.A.; Ferrari, B. *Int. J. Peptide Protein Res.* **1983**, *22*, 539-548.
29. Sabesan, S.; Bock, K.; Lemieux, R.U. *Can. J. Chem.* **1984**, *62*, 1034-1045.
30. Springer, G.F. *Science* **1984**, *224*, 1198-1206.
31. Dill, K.; Ferrari, B.; Lacombe, J.M.; Pavia, A.A. *Carbohydr. Res.* **1981**, *101*, 330-334.
32. Freeman, R.; Kempsell, S.P.; Levitt, M.H. *J. Magn. Reson.* **1979**, *34*, 663-667.
33. Tvaroška, I.; Hricovíni, M.; Petráková, E. *Carbohydr. Res.* **1989**, *189*, 359-362.
34. For a recent review, see Juarishi, E.; Cuevas, G. *Tetrahedron* **1992**, *48*, 5019-5087.
35. Nishida, Y.; Hori, H.; Ohrui, H.; Meguro, H. *J. Carbohydr. Chem.* **1988**, *7*, 239-250.
36. Tagaki, S.; Jeffrey, G.A. *Acta Cryst.* **1979**, *B35*, 902-906.
37. Forsén, S.; Hoffman, R.A. *J. Chem. Phys.* **1963**, *39*, 2892-2901.
38. Wu, G.D.; Serrianni, A.S.; Barker, R. *J. Org. Chem.* **1983**, *48*, 1750-1757.
39. Koole, L.H.; Lanters, E.J.; Buck, H.M. *J. Am. Chem. Soc.* **1984**, *106*, 5451-5457.
40. Goodford, P.J. *J. Med. Chem.* **1984**, *27*, 557-570; **1985**, *28*, 849-857.

(*Received in USA* 21 *July* 1993; *accepted* 7 *October* 1993)